Title

Soil phosphorus cycling across a 100-year deforestation chronosequence in the Amazon rainforest

Journal

Global Change Biology, 30(1)

ISSN

1354-1013

Authors

Xu, Suwei

Gu, Chunhao

Rodrigues, Jorge LM

et al.

Publication Date

2024

DOI

10.1111/gcb.17077

Peer reviewed

Received: 8 June 2023 | Revised: 9 November 2023 | Accepted: 13 November 2023

DOI: 10.1111/gcb.17077

Global Change Biology WILEY

RESEARCH ARTICLE

Soil phosphorus cycling across a 100-year deforestation chronosequence in the Amazon rainforest

Suwei Xu[1] | Chunhao Gu[2] | Jorge L. M. Rodrigues[3,4] | Chongyang Li[1] | Brendan Bohannan[5] | Klaus Nüsslein[6] | Andrew J. Margenot[1,7]

[1]Department of Crop Sciences, University of Illinois at Urbana-Champaign, Urbana, Illinois, USA

[2]Department of Plant and Soil Sciences, Delaware Environmental Institute, University of Delaware, Newark, Delaware, USA

[3]Department of Land, Air and Water Resources, University of California Davis, Davis, California, USA

[4]Environmental Genomics and Systems Biology Division, Lawrence Berkeley National Laboratory, Berkeley, California, USA

[5]Institute of Ecology and Evolution, University of Oregon, Eugene, Oregon, USA

[6]Department of Microbiology, University of Massachusetts Amherst, Amherst, Massachusetts, USA

[7]Agroecosystem Sustainability Center (ASC), Institute for Sustainability, Energy and Environment (iSEE), University of Illinois at Urbana-Champaign, Urbana, Illinois, USA

Correspondence
Andrew J. Margenot, Department of Crop Sciences, University of Illinois at Urbana-Champaign, Urbana, IL 61801, USA.
Email: margenot@illinois.edu

Funding information
National Institute of Food and Agriculture, Grant/Award Number: 2009-35319-05186

Abstract

Deforestation of tropical rainforests is a major land use change that alters terrestrial biogeochemical cycling at local to global scales. Deforestation and subsequent reforestation are likely to impact soil phosphorus (P) cycling, which in P-limited ecosystems such as the Amazon basin has implications for long-term productivity. We used a 100-year replicated observational chronosequence of primary forest conversion to pasture, as well as a 13-year-old secondary forest, to test land use change and duration effects on soil P dynamics in the Amazon basin. By combining sequential extraction and P K-edge X-ray absorption near edge structure (XANES) spectroscopy with soil phosphatase activity assays, we assessed pools and process rates of P cycling in surface soils (0–10 cm depth). Deforestation caused increases in total P (135–398 mg kg^{-1}), total organic P (P_o) (19–168 mg kg^{-1}), and total inorganic P (P_i) (30–113 mg kg^{-1}) fractions in surface soils with pasture age, with concomitant increases in P_i fractions corroborated by sequential fractionation and XANES spectroscopy. Soil non-labile P_o (10–148 mg kg^{-1}) increased disproportionately compared to labile P_o (from 4–5 to 7–13 mg kg^{-1}). Soil phosphomonoesterase and phosphodiesterase binding affinity (K_m) decreased while the specificity constant (K_a) increased by 83%–159% in 39–100y pastures. Soil P pools and process rates reverted to magnitudes similar to primary forests within 13 years of pasture abandonment. However, the relatively short but representative pre-abandonment pasture duration of our secondary forest may not have entailed significant deforestation effects on soil P cycling, highlighting the need to consider both pasture duration and reforestation age in evaluations of Amazon land use legacies. Although the space-for-time substitution design can entail variation in the initial soil P pools due to atmospheric P deposition, soil properties, and/or primary forest growth, the trend of P pools and process rates with pasture age still provides valuable insights.

KEYWORDS
Amazon, chronosequence, deforestation, phosphatase, phosphorus, phosphorus fractionation, reforestation, XANES

1 | INTRODUCTION

Phosphorus (P) limitation in highly weathered soils with low P stocks and high P fixing capacity constrains the primary productivity of tropical forests (Malhi et al., 2008; Yao et al., 2018). This is exemplified by the Amazon rainforest, the largest tropical rainforest in the world with an estimated extent of 6.2 million km^2 (Durrer et al., 2021; Malhi et al., 2008). Evidence suggests that P is predominantly a limiting nutrient in the Amazon (Cunha et al., 2022; Dalling et al., 2016; Yao et al., 2018). Expanding agricultural frontiers have driven deforestation of native Amazon forest (Chavarro-Bermeo et al., 2022; Durrer et al., 2021), a land use change that disrupts nutrient and water cycles, and in particular P cycling (Asner et al., 2004; Chavarro-Bermeo et al., 2022; Garcia-Montiel et al., 2000). As of 2013, approximately 750,000 km^2 of primary forest in the Amazon Forest region had been converted to agriculture (i.e., pasture, row cropping) (Neill et al., 2001; Nogueira et al., 2015). Driven in large part by declining P availability in pastures and subsequently lowered productivity, nearly half of the pastures are abandoned by farmers within 5–15 years (Aguiar et al., 2016; Nagy et al., 2017). Abandonment of pastures entails secondary forest development, growth of which is also generally P limited (Lawrence & Schlesinger, 2001; Wright, 2019). Impacts of deforestation and subsequent reforestation (i.e., secondary forest succession) in the Amazon basin on soil P cycling in these already P-limited systems are likely to influence future agroecosystem functions, with limited productivity and decelerated carbon (C) cycling (Durrer et al., 2021; McGrath et al., 2001; Nagy et al., 2017).

In the Amazon rainforest, conversion of primary forest to pasture has been variously reported to result in decreases (Asner et al., 2004; Garcia-Montiel et al., 2000), increases in total P stocks (Garcia-Montiel et al., 2000), or no changes (Chavarro-Bermeo et al., 2022; McGrath et al., 2001) in soil total P concentrations in surface depths. This can be attributed to the different vegetation species, land use management practices, different soil types across studies, and potentially insufficiently long chronosequences that do not span multidecadal scales at which P cycling shifts may occur (Garcia-Montiel et al., 2000; Hamer et al., 2013; McGrath et al., 2001). Beyond total soil P, differences in pool sizes reflect bioavailability of this limiting element that are relevant to understanding deforestation and reforestation dynamics. Generally, it is expected that the labile P pools increase immediately after the forest conversion to pasture (Garcia-Montiel et al., 2000; McGrath et al., 2001) since the slash-and-burn process deposits former biomass P onto the soil surface and increases soil pH via ash, which can stimulate organic P (P_o) mineralization by phosphatases and reduce P sorption (McGrath et al., 2001; Sanchez, 1977).

Contradictory responses of P pools to land use conversion in long-term chronosequences may reflect the complex response of soil P cycling components (e.g., soil phosphatase catalysis of P mineralization, soil pH) to land use change. For instance, following Amazon forest conversion to pasture, the labile inorganic P (P_i) pool either decreased with pasture age within 12–25 years (Asner et al., 2004; Chavarro-Bermeo et al., 2022) or increased in the initial 4–5 years before decreasing thereafter until 50 years (Garcia-Montiel et al., 2000). Decreasing labile P with pasture age is expected since labile P can be transformed into more recalcitrant P fractions (i.e., iron- and/or aluminum-associated P ((Fe + Al)-P) or calcium-bounded P (Ca-P)) via adsorption and precipitation (Lawrence & Schlesinger, 2001). Deposition of calcium (Ca)-rich ash may initially increase Ca-P, which is likely to dissolve over time in the acidic soils common in the Amazon basin.

Soil P_o cycling plays a key role in P availability in weathered soils such as the Amazon basin (Reed et al., 2011), and is likely to be impacted by land use change. Changes in soil organic carbon (SOC) may entail a concomitant change in P_o, due to (1) the dominance of soil P immobilization with a high soil C:P_o ratio (Arenberg & Arai, 2021); and (2) a constrained C:P_o (i.e., increased total C with a constant ratio entails increased P_o). Reforestation, though less evaluated, is hypothesized to entail shifts in soil available P pools to the P_o fraction in tropical secondary forests due to an increase in litter deposition (Brown & Lugo, 1990). As soil phosphatases catalyze depolymerization and mineralization of P_o, assaying the activities of these hydrolytic enzymes can provide insight to shifts of labile P and P_o pool responses to land use change. Phosphomonoesterase (PME) and phosphodiesterase (PDE), the two major phosphatase classes in soils, work in concert to yield bioavailable orthophosphate (Chavarro-Bermeo et al., 2022; Soltangheisi et al., 2019). Contradictory results on PME activity response to forest-to-pasture conversion range from increases (Soltangheisi et al., 2019) to decreases (Chavarro-Bermeo et al., 2022; Silva-Olaya et al., 2021), and no studies have considered PDE, despite its proposed rate-limiting influence on P mineralization (Turner & Haygarth, 2005). Enzyme kinetic parameters of maximum catalysis rate (V_{max}) and the substrate concentration that yields half of V_{max} (K_m) provide more information on phosphatases as process rate indicators than enzyme activity assayed at a single substrate concentration (German et al., 2011; Stone & Plante, 2014). Given the general stoichiometric scaling of phosphatase activities with total P_o (Soltangheisi et al., 2019), to the extent that P_o changes with deforestation, both V_{max} and K_m are also expected to shift with similar directionality.

To quantitatively evaluate how deforestation and subsequent secondary forest growth following abandonment may alter soil P cycling in the Amazon basin, we evaluated changes in soil P pool sizes (sequential chemical extraction), molecular speciation (P K-edge X-ray absorption near edge structure [XANES] spectroscopy), and potential transformation rates (phosphatase V_{max} and K_m). Leveraging a well-characterized and replicated 100-year chronosequence of primary forest-to-pasture conversion and a 13-year-old secondary forest (Durrer et al., 2021; Paula et al., 2014; Rodrigues et al., 2013), we aimed to quantify the effect of land use changes on soil P pool sizes and process rates. Specifically, we hypothesized (1) soil total P and pools of labile P, (Fe + Al)-P, and Ca-P would initially increase following the slash-and-burn conversion of forest to pasture, and both total P and (Fe + Al)-P gradually increase while would labile P and Ca-P decrease with pasture age; (2) given that SOC increases with

pasture age (Durrer et al., 2021), soil P_o would also increase with pasture age, though C:P_o plasticity could entail proportionately different changes in P_o; (3) the expected increase in soil P_o and decrease in labile P with pasture age would lead to an increase in V_{max} and K_m of soil phosphatases; and (4) for reforestation, soil P cycling variables would revert to similar pool sizes or rates as those observed in primary forests within 13 years of pasture abandonment.

2 | MATERIALS AND METHODS

2.1 | Sites description, and experimental design

The study was conducted at the Amazon Rainforest Microbial Observatory (ARMO), Fazenda Nova Vida ranch (10°10′5″ S and 62°49′27″ W), in the state of Rondônia, Brazil (Figure S1) to assess ecosystem responses to land use change (Cerri et al., 2004; Durrer et al., 2021; Neill, Cerri, et al., 1997). This state is one of the regions in the Amazon basin most impacted by agriculture, with the highest forest loss (28.5%) among Brazilian states. The state of Rondônia together with the states of Mato Grosso and Pará collectively accounted for more than 85% of all Amazon deforestation from 1996 to 2005 (INPE, 2011). Due to development of highways that enabled logging and agriculture expansion, significant deforestation in Amazon started in 1970s (Danielson & Rodrigues, 2022; Leite et al., 2011). Deforestation in the state of Rondônia accounted for over 8000 km^2 of forest loss by 1980, which rose to 28,000 km^2 by 1985 (Malingreau & Tucker, 1988). Deforestation rates in the state of Rondônia increased in the early 1990s (Pedlowski et al., 1997), peaked in 1995 at approximately 5000 $km^2 year^{-1}$, and was further facilitated by the arrival of mechanized agriculture in 2000s (Brown et al., 2004). As of 2011, approximately 51,766 km^2 or 22% of the state of Rondônia had been deforested (Butt et al., 2011). The climate is tropical humid with a mean annual temperature of 25.5°C and a historical mean annual precipitation of 2200 mm distributed over a well-defined wet season from September to May (Bastos & Diniz, 1982). The primary forest is classified as upland humid evergreen ombrophiles (Pires & Prance, 1985).

The sampling area has served as a model for studying forest-to-pasture conversion due to staggered times of primary forest conversion to pasture over the last century, which enables characterizing long-term changes in soil P cycling in the present study. Representative of practices in the region, pastures were developed by slash-and-burn clearing followed by seeding with *Brachiaria brizantha* (Cerri et al., 2004) as a forage for cattle, stocked at 1 cow ha^{-1}. Pastures were burned for weed control as needed every 4–10 years and did not receive inputs (e.g., fertilizers, lime, herbicides) (Neill, Melillo, et al., 1997). Secondary forest was established when 7- to 10-year-old pastures were abandoned due to insufficient grass regeneration and increasing weed invasion (Paula et al., 2014). The secondary forest vegetation cover at our study site is comprised of ~63% herbaceous species (including pasture grasses), 15%–18% woody tree species, and ~12% palm species (Feigl et al., 2006). We carefully selected specific plot locations for primary and secondary forests as well as pastures to be situated on the same soil type, Kandiudults (USDA Soil Taxonomy) or red-yellow podzolic Latosols (World Reference Base for Soil Resources), with sandy clay loam texture (Feigl et al., 2006; Neill, Melillo, et al., 1997; Rodrigues et al., 2013) formed on parent material of pre-Cambrian granite (Neill et al., 2011). As for any observational chronosequence study, we assume that all land uses and durations differ primarily in age, which in our case also assumes similar P pool sizes and process rates prior to forest-to-pasture conversion (De Palma et al., 2018; Miyanishi & Johnson, 2007). While the space-for-time substitution has shortcomings (Damgaard, 2019), this site offers a rare opportunity to understand a land use change that has expanded contemporaneously with the chronosequence duration.

2.2 | Soil sampling

Sampling sites from two primary forests and four pastures represented a chronosequence of forest-to-pasture conversion from initial deforestation in 1911 (100y), 1972 (39y), 1987 (24y), and 2004 (7y); and a secondary forest corresponding to pasture abandonment in 1998 (Figure S1). The secondary forest was under at least 10 years of pasture production before abandonment. Soils were sampled at the end of the 2011 austral summer. Surface litter was removed and soils were sampled to 10 cm depth with a 5 cm diameter sterile PVC tube, for a total of three samples for each land use and pasture age (Paula et al., 2014; Rodrigues et al., 2013). Prior to analyses, soils were air-dried at 25°C and gently hand-ground to pass a <2 mm sieve.

2.3 | Soil properties

Soil pH was measured by adding water to the soil with a ratio of 1:5 (m/v) and incubating for 1 h to match soil phosphatase activity assay parameters. Soil texture was measured using the modified pipette method (Kettler et al., 2001). Total soil C and total soil nitrogen were determined by dry combustion using an ECS 4010 CHNSO Analyzer (Costech, Valencia, CA). Carbonates were not detected gravimetrically by hydrochloric acid addition, enabling total soil C to be interpreted as SOC. Mehlich-3 P was determined on air-dried soils according to Mehlich (2008).

Pedogenic iron (Fe) and aluminum (Al) minerals in soils are strongly related to soil P due to the adsorption of P_i and P_o compounds on these mineral surfaces. To evaluate potential changes in pedogenic Fe and Al minerals, poorly crystalline and well-crystallized Fe and Al minerals were determined by sequential extraction using ammonium oxalate solution followed by sodium dithionite–citrate solution, respectively (Gu et al., 2019). First, the extraction using acidified (pH 3.0) ammonium oxalate solution was conducted using modified procedures as described in Sparks et al. (1996). Oxalate extractable Fe, Al and P (Fe_{ox}, Al_{ox}, P_{ox}) were derived from organic

complexes and poorly crystalline Fe (e.g., ferrihydrite) and aluminosilicates (e.g., allophane and imogolite), and the dithionite–citrate extractable Fe, Al and P (Fe_{di}, Al_{di} and P_{di}) represent highly crystalline Fe and Al minerals (e.g., goethite and gibbsite). The concentrations of Fe_{ox}, Al_{ox}, Fe_{di}, Al_{di}, P_{di}, and P_{ox} were measured via inductively coupled plasma optical emission spectroscopy (ICP-OES). The ratio of Fe_{di} to the sum of Fe_{ox} and Fe_{di} ($Fe_{di}/(Fe_{ox}+Fe_{di})$) was calculated as an indicator of the degree of soil weathering. All extractions were conducted at 24°C with 10% of soil samples extracted in triplicates for quality control (QC). The relative standard deviations for all QC samples were <10%, and analytical errors for ICP-OES measurements were <5.8%.

2.4 | Total P and P fractionation

Total P was determined on 2 mm sieved soils digested with nitric acid and hydrogen peroxide at 105°C for 24 h (White Jr & Douthit, 1985) and orthophosphate quantified using phosphomolybdate colorimetry (Murphy & Riley, 1962).

Soil P distribution was assessed by sequential extraction of P based on Hedley et al. (1982). Soils were sequentially extracted in triplicate by the Hedley fractionation using an anion-exchange membrane (AEM) strip in distilled water, 0.5 mol L^{-1} $NaHCO_3$ (pH 8.5), 0.1 m L^{-1} NaOH, and 1 mol L^{-1} HCl. A negative control (no soil) and soil standard were also included. All extractions were performed by 16 h of horizontal shaking (120 rev min^{-1}). An AEM strip (1 × 4 cm, VWR International, West Chester, PA) was loaded with carbonate as the counterion and used to extract soils in distilled water. Resin extractable inorganic P (Resin-P_i) was desorbed from the membranes by shaking for 1 h in 0.25 mol L^{-1} H_2SO_4. All other extracts were centrifuged (8000 *g*, 15 min) and an aliquot was decanted for analysis. P_o in the distilled water used to extract AEM-P_i was quantified as P_i following acid–persulfate digestion (80°C, 16 h) by phosphomolybdate colorimetry (Murphy & Riley, 1962) at 882 nm. For NaOH aliquots, OM was precipitated with 1.2 mol L^{-1} H_2SO_4 to avoid interference with colorimetry. For $NaHCO_3$ and NaOH extractions, aliquots were neutralized and analyzed for P_i and total P (P_t). P_t was determined as P_i following acid–persulfate digestion. P_o was estimated as the difference between total and inorganic P ($P_o = P_t - P_i$). Fractions were quantified as mg P kg^{-1} soil. Total soil P_o was calculated as the sum of H_2O-P_o, $NaHCO_3$-P_o and NaOH-P_o. Labile P_i was calculated as the sum of AEM-P_i, and $NaHCO_3$-P_i.

2.5 | Phosphorus X-ray absorption structure spectroscopic analysis

Phosphorus K-edge XANES spectra of the soils that were further ground to <0.5 mm diameter were collected in fluorescence mode at the SXRMB station of the Canadian Light Source (Saskatoon, Canada). A Si(111) double-crystal monochromator with a four-element Si(Li) drift detector was used with energy calibration using $AlPO_4$. Samples were thinly spread across a double-sided carbon tape using one to three scans to maximize the signal-to-noise ratio. The energy range for all the scans was 2119.5–2210 eV with the following regions and step sizes: 2119.5–2143 eV: 2 eV; 2143–2175 eV: 0.15 eV; and 2175–2210 eV: 0.75 eV. The dwelling time of each step varied from 1 to 4 s, depending on total P concentrations determined beforehand (see Section 2.4). ATHENA software was used for background removal, normalization, and linear combination fitting (LCF) over 2140–2180 eV.

Five reference spectra were used for LCF analysis, as described by Gu et al. (2020): phytate acid (sodium salts), dicalcium phosphate ($Ca(HPO_4)$), poorly crystalline berlinite ($AlPO_4$), and phosphate adsorbed on amorphous $Al(OH)_3$ (AAH) and ferrihydrite, which represent soil P_o, Ca-P, Al-P, and Fe-P well (Figure S2a). The spectrum of phytate was reported by Gu et al. (2019). The spectrum of P adsorption on AAH (AAH-P) was reported previously and the adsorption was conducted by reacting 0.5 mM phosphate with 2 g L^{-1} AAH. Dicalcium phosphate ($Ca(HPO_4)$) was purchased from Sigma-Aldrich. The two-line ferrihydrite was synthesized using the method described in Zhu et al. (2013) while amorphous $AlPO_4$ was synthesized according to Xiaoming Wang et al. (2019). Phosphate adsorption on ferrihydrite experiments was conducted by reacting 1 mM phosphate with 2 g L^{-1} ferrihydrite in 0.1 M $NaNO_3$ background substrate at pH 5.0 for 3 day at room temperature (~21°C). Solids were filtered and air-dried at ~21°C for 24 h and finely ground prior to XANES data collection.

2.6 | Soil phosphatase assays

To evaluate the impacts of land use and agricultural management on direct drivers of P_o transformations, we characterized the V_{max} and K_m of soil PME (Enzyme Commission 3.1.3) and PDE (EC 3.1.4.1). Measured catalysis rates (i.e., activities) in soils represent potential maximum rates of P_o transformation (Nannipieri et al., 2017), from phosphodiester forms (e.g., nucleic acids, phospholipids) to phosphomonoester forms by PDE, and from phosphomonoester forms to bioavailable orthophosphate by PME. Soil PME catalytic activities were assayed in duplicate for each soil sample in water at final substrate concentrations of 1, 3, 5, 10, 30, and 50 mmol L^{-1} *para*-nitrophenyl phosphate disodium g^{-1} soil. Similarly, soil PDE assays were performed in duplicate for each soil sample in water at 1, 3, 5, 10, 30, and 50 mmol L^{-1} *bis-para*-nitrophenyl phosphate g^{-1} soil. Preliminary tests indicated *para*-nitrophenyl phosphate disodium increased matrix pH whereas *bis-para*-nitrophenyl phosphate drastically acidified the assay solution; therefore, the former substrate aqueous solution was adjusted with 1% HCl to a pH close to the bulk soil pH (difference within 0.3 unit), whereas the latter substrate was adjusted with 10% NaOH to the target pH (Table S1).

To calculate the catalysis kinetic parameters of V_{max} and K_m, phosphatases were assayed using 0.50 g of oven-dried soil equivalent and 2.5 mL aqueous substrate mixture incubated for 1 h at 37°C Reactions were terminated by the addition of 2 mL 0.1 mol L^{-1} Tris

(pH 12.0), and 0.5 mL 2 mol L^{-1} $CaCl_2$. The mixture was centrifuged (22,000 *g*) to obtain a clear supernatant in which the product *para*-nitrophenol (*p*NP) was quantified with a 96-well microplate reader (BioTek, Winooski, VT) using absorbance at 410 nm. The absorbance of negative controls (i.e., substrate with no soil) was subtracted from the absorbance of soil assays to account for the non-enzymatic hydrolysis of substrate during the incubation (Neal et al., 1981; Turner et al., 2002). Enzyme activities were corrected for soil-specific dissolved organic matter by subtracting absorbance at 410 nm of a soil-only control subjected to incubation and termination. Additionally, the potential sorption of *p*NP by soil components was corrected by measuring the recovery of *p*NP in the same assay conditions using a relevant *p*NP concentration (1 mmol L^{-1} g^{-1} soil) to ensure accurate kinetic characterization (Cervelli et al., 1973; Margenot et al., 2018). A non-linear Michaelis–Menten kinetic model was fitted using the Enzyme Kinetics Module add-on in SigmaPlot 14.0 to derive V_{max} and K_m. The enzyme specificity constant (K_a) was calculated based on the ratio of V_{max} and K_m values.

2.7 | Statistical analysis

All statistical analyses were performed using the RStudio Desktop 1.4. Significant differences between different land uses and durations were identified at $p < .05$. One-way ANOVA and Tukey's HSD test were performed for all measured parameters since samples were collected in a chronosequence. The effects of land use (forests [primary and secondary forest] vs. pastures [7y, 24y, 39y, 100y]) on the soil P variables, including total P and P fractions, were analyzed by Student's *t*-test. Relationships between pasture age and previous variables were assessed by Spearman correlation coefficients.

3 | RESULTS

3.1 | Soil physiochemical properties

Soils across land use type and duration expressed similiar sandy clay loam texture. Soil organic C concentration was positively associated with pasture age (Spearman coefficient (ρ) = .85, $p < .001$) (Table 1; Table S5), and was similiar in primary (7.9 g kg^{-1}) and secondary (9.5 g kg^{-1}) forests. Soil Mehlich-3 P exhibited a similar trend as total P, with lower Mehlich-3 concentrations in forests (primary and secondary) and higher concentrations in older pastures (39 and 100y). Middle-aged (39y) pasture had the greatest Mehlich-3 P (9.3 ± 4.7 mg kg^{-1}) and total P (549 ± 325 mg kg^{-1}), albeit with relatively large variances. Mehlich-3 P increased with pasture age (ANOVA, $p < .05$) (Table 1; Table S6), though less strongly than SOC ($\rho = .61$, $p < .05$) (Table S5). Forests had significantly lower total P than pastures (7, 24, 39, and 100y) ($p < .05$) (Table S7), and soil total P was positively correlated with pasture age ($\rho = .84$, $p < .001$) (Table S5). The C:P_o ratio ranged from 143 to 503 (Table 1) and were similar among all land uses and durations. Soils were moderately or slightly acidic, varying from 6.10 to 6.19 in pastures and slightly higher in primary forests (6.46 ± 0.39) but lower in the secondary forest (5.61 ± 0.02).

Sequential extraction of oxalate and dithionite–citrate extractable Fe, Al, and P showed different trends along with pasture age (Figure 1). The concentration of Fe_{ox} increased significantly with pasture age from 14 to 47 mg kg^{-1}, whereas Al_{ox} remained stable across pasture age (Figure 1A). Both Fe_{ox} and Al_{ox} in primary and secondary forests were similar (Figure 1B). P_{ox} increased with pasture age from 0.3 to 2.6 mg kg^{-1} (Figure 1A), and was similar in secondary (0.40 ± 0.08 mg kg^{-1}) and primary (0.38 ± 0.15 mg kg^{-1}) forests (Table S7). Fe_{di} and Al_{di} exhibited similar trends as P_{ox} with pasture age (Figure 1B). The 7y pasture had the highest concentrations for both Fe_{di} (214 ± 24 mg kg^{-1}) and Al_{di} (33 ± 5 mg kg^{-1}). Fe_{di} in the secondary forest was significantly higher than in primary forests, whereas Al_{di} in primary and secondary forests were similar. P_{di} was only higher for older pastures from 39 to 100y (Figure 1B). Along with pasture age from 0 to 100 years, the $Fe_{di}/(Fe_{ox}+Fe_{di})$ ratio decreased from 0.87 ± 0.03 to 0.66 ± 0.02 ($p < .05$) (Figure 1C). The $Fe_{di}/(Fe_{ox}+Fe_{di})$ ratio was similar within forests, but higher for forests relative to pastures ($p < .05$) (Table S7).

3.2 | P K-edge XANES spectroscopy

The proportions of P species identified by XANES were not influenced by land use type or pasture age (Figure 2; Figure S2). Soil P fractions characterized by XANES were similar (Figure 2; Table S6), and dominated by (Fe + Al)-P (39%–53%) and P_o (39%–49%)

TABLE 1 Soil physiochemical properties (0–10 cm depth) from a 100-year deforestation chronosequence in the Brazilian Amazon, in which primary forests (PFs) were converted to pastures. Also included is a 13-year-old secondary forest (SF) site established by reforestation of abandoned pastures. Different letters among sites indicate significant differences (Tukey's HSD, $p < .05$).

Sites	pH	Mehlich-3 P (mg kg^{-1})	SOC (g kg^{-1})	Total P (mg kg^{-1})	C:P_o ratio
PF	6.46 (0.39)a	5.0 (1.0)ab	7.9 (2.3)d	134 (40)b	461 (236)a
7y	6.14 (0.19)ab	3.3 (0.6)b	11.6 (1.2)bcd	147 (15)b	321 (108)a
24y	6.10 (0.04)ab	5.0 (1.0)ab	17.1 (0.7)ab	220 (19)ab	253 (14)a
39y	6.19 (0.53)ab	9.3 (4.7)a	16.4 (0.4)abc	549 (325)a	503 (288)a
100y	6.15 (0.29)ab	7.7 (1.2)ab	23.4 (5.5)a	398 (60)ab	143 (47)a
SF	5.61 (0.02)b	5.0 (1.0)ab	9.5 (1.3)cd	193 (50)ab	234 (105)a

Abbreviations: C:P_o ratio, carbon to organic phosphorus ratio; SOC, soil organic carbon.

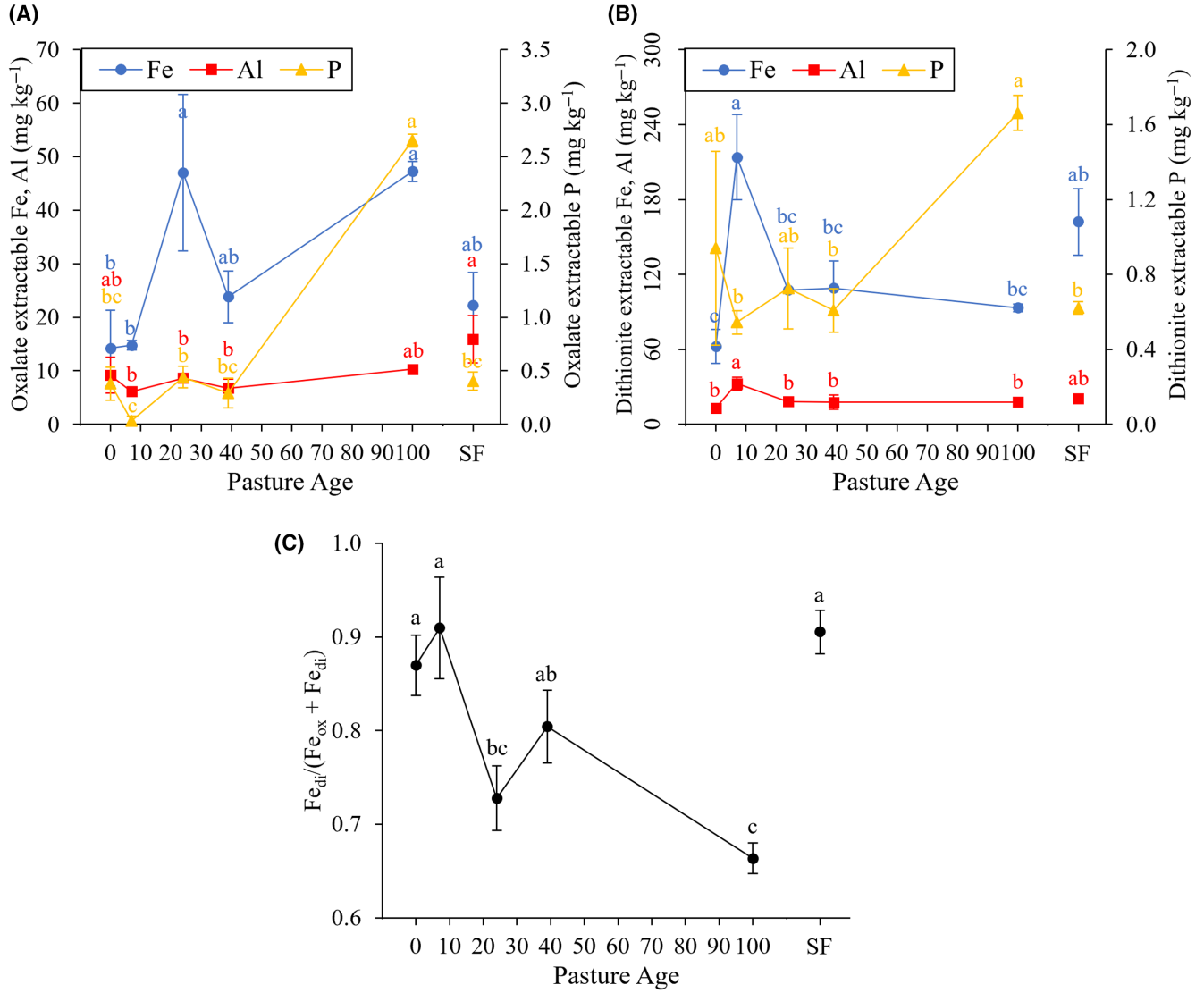

FIGURE 1 Soil concentrations (mg kg^{-1}) of Fe, Al, and P sequentially extracted by (A) ammonium oxalate and (B) sodium dithionite–citrate, and (C) the soil weathering degree index as indicated by the concentration ratio of dithionite–citrate extractable Fe (Fe_{di}) to the sum of oxalate extractable Fe (Fe_{ox}) and Fe_{di} [$Fe_{di}/(Fe_{ox}+Fe_{di})$] of soils (0–10 cm depth) across a 100-year deforestation chronosequence in the Brazilian Amazon, in which primary forests (0 year) were converted to pasture. Also included is a 13-year-old secondary forest (SF) site established by the reforestation of abandoned pastures. The standard deviations were calculated from $n = 3$ sites, indicating the within-site variations. Different letters among pasture age indicate significant differences (Tukey's HSD, $p < .05$).

(Figure 2). Soil Ca-P was approximately 13%–15% of total P across primary forests and pastures, but lower and not detectable in the secondary forest (~3%) due to the error of P K-edge XANES (10%). The reduced χ^2 of .005 indicated an excellent fit using reference spectra of P standards (Table S2).

3.3 | Total P_i, P_o, and P fractionation

Soil total P, P_i, and P_o increased after deforestation (Figure 3; Table S4). Total P varied less (fourfold) than residual P (sixfold), and both exhibited similar post-deforestation trends (Figure 3A). Soil P_o varied more (eightfold) than P_i (fourfold), and the concentrations of both P_i ($\rho = .55$, $p < .05$) and P_o ($\rho = .79$, $p < .001$) increased with pasture age (Table S5), and were similar in primary and secondary forests (Figure 3A). Soil P composition exhibited a greater proportion of P_o (14%–42%) than P_i (7%–29%) (Figure 3B), with the lowest P_o and Pi proportions in the 39y pasture due to the high residual P content (79%) and the highest percentages in the 100y pasture (Figure 3B). The proportion of total P as P_i and P_o were similar between primary and secondary forests (Figure 3B).

Operationally defined P_i fractions showed similar trends along with pasture age (Figure 3C,D). Soil P fraction concentrations decreased in the order of NaOH-P_i (17–80 mg kg^{-1}) > labile P_i (3–17 mg kg^{-1}) > HCl-P_i (1–17 mg kg^{-1}). No significant difference was observed from primary forests to mid-age (39y) pasture, and between primary and secondary forests for all three P_i fractions (Figure 3C). The highest concentrations for all P_i fractions were in the

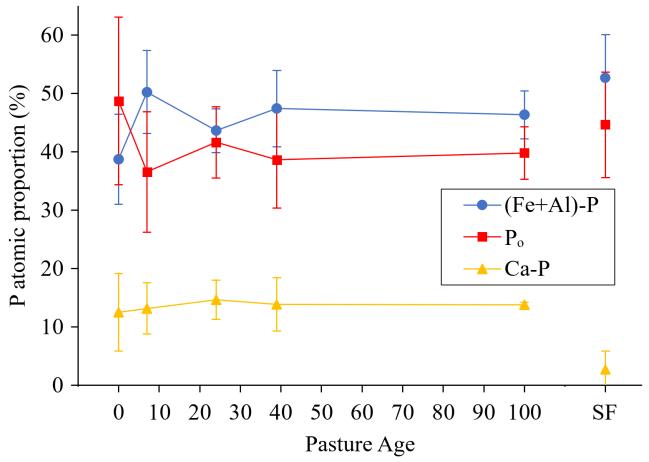

FIGURE 2 The proportion (% atom contribution) of P species, including Fe- and Al-associated P [(Fe + Al)-P], organic P (P_o), and Ca-associated P (Ca-P), quantified by P X-ray absorption near edge structure spectroscopy in soils (0–10 cm depth) from a 100-year deforestation chronosequence in the Brazilian Amazon, in which primary forests (0 year) were converted to pastures varying in age from 7 to 100 years at the time of sampling. Also included is a 13-year-old secondary forest (SF) site established by reforestation of abandoned pasture. Standard deviations was calculated from $n = 3$ sites, indicating the within-site variation of each P species. Tukey's HSD tests indicated no significant difference within each P fraction among pasture age.

100y pasture which was significantly higher than others. Increases with pasture age occurred for NaOH-P_i ($\rho = .55$, $p < .05$) (Table S5) and HCl-P_i ($\rho = .70$, $p < .01$) (Table S5), and HCl-P_i was also higher in pastures than in forests ($p < .1$) (Table S7). The relative percentage of P_i fractions in total P_i remained relatively constant across land uses and durations (Figure 3D), dominated by NaOH-P_i (~70%–79%) and labile P_i (~11%–17%). Only the proportion in total P_i as HCl-P_i in primary forests (~6%) was lower than in the 100y pasture (~15%) (Figure 3D).

Similar to P_i fractions, concentrations of P_o fractions increased with pasture age (Figure 3E,F). Pool sizes of P_o fractions were in a sequence of NaOH-P_o (10–148 mg kg^{-1}) > HCO_3-P_o (4–13 mg kg^{-1}) > H_2O-P_o (4–7 mg kg^{-1}) for all land uses and durations. Similar to P_i fractions, P_o fractions also remained stable from primary forests to 39y pasture and increased with pasture age thereafter to 100y. P_o fractions in the 100y pasture were higher than in other pastures and forests, and similar in primary versus secondary forests (Figure 3E). Both HCO_3-P_o ($\rho = .89$, $p < .001$) and NaOH-P_o ($\rho = .76$, $p < .001$) were positively associated with pasture age (Table S5), and NaOH-P_o was also higher in pastures than forests ($p < .05$) (Table S7). Expressed as a proportion of total P_o, P_o fractions exhibited distinct trends with pasture age and reforestation to the secondary forest (Figure 3F): NaOH-P_o was the dominant P_o pool (47%–88%) and generally increased with pasture age, with the lowest percentage in primary forests and the highest in 100y pastures (Figure 3F). HCO_3-P_o% (8%–24%) remained stable while H_2O-P_o% (4%–29%) decreased with pasture age (Figure 3F). The H_2O-P_o% was higher in primary forests (29%) than in other pastures and the secondary forest (4%–11%).

3.4 | Soil phosphatase kinetic properties

The response of phosphatase V_{max} and K_m was also influenced by deforestation and reforestation (Figure 4A,B). The V_{max} for both PME and PDE were similar among all land uses and durations (Figure 4A). Maximum velocity was 10–18 μmol g^{-1} h^{-1} for PME, fivefold higher than 2–4 μmol g^{-1} h^{-1} for PDE (Figure 4A). The V_{max} of PDE was positively correlated with pasture age ($\rho = .52$, $p < .05$) (Table S5), and was higher in pastures than in primary and secondary forests ($p < .01$) (Table S7). The K_m was 7–15 mmol g^{-1} for PME and 7–19 mmol g^{-1} for PDE (Figure 4B). For PME, K_m generally decreased with pasture age from 0 to 100 years ($\rho = -.65$, $p < .01$) (Table S5). The K_m of PDE was uniquely highest in the youngest pasture (7y) relative to other land uses and durations (Figure 4B), and PME and PDE K_m in primary and secondary forests were similar. The K_a increased with pasture age for PME ($\rho = .86$, $p < .001$) and PDE ($\rho = .67$, $p < .01$) (Table S5). The PME K_a increased with pasture age until 39 years, and then remained stable (Figure 4C), and was 2.6-fold greater in 39y pasture relative to primary forests. In contrast, K_a of PDE (0.2–0.5 μmol h^{-1} mmol^{-1}) was similar among land uses and durations. Although PME and PDE K_a were similar between primary and secondary forests, PME K_a was higher under pasture than in forests ($p < .01$) (Table S7).

4 | DISCUSSION

4.1 | Soil total P and P_i pool size change with time since deforestation

Similar soil P pool sizes among the youngest pasture and primary forests indicate that the 7 years of the youngest pasture did not capture expected changes in soil after slash-and-burn conversion. This is consistent with soil pH being similar among pastures, as increases in soil pH following the burning of forests are hypothesized to be a major driver of soil P change. Following the slash-and-burn conversion, soil total P and labile P tend to transiently increase due to pyromineralization and ash deposition (Lawrence & Schlesinger, 2001), with reversion of these pool sizes to primary forests within 3–13 years (Chavarro-Bermeo et al., 2022; Garcia-Montiel et al., 2000). At our site, soil total P at 0–10 cm depth remained consistent in the first 7 years of pasture following deforestation and increased in 100y pasture, potentially a result of pasture grass uptake from subsurface depths and deposition at the surface via litter (Friesen et al., 1997; Han et al., 2021). Similarly, occasional burning to maintain pasture integrity could lead to surface deposition of P acquired at subsurface depths. A similar increase in soil total P in a 41-year deforested pasture with periodic burning compared to the primary forests was also reported (Garcia-Montiel et al., 2000).

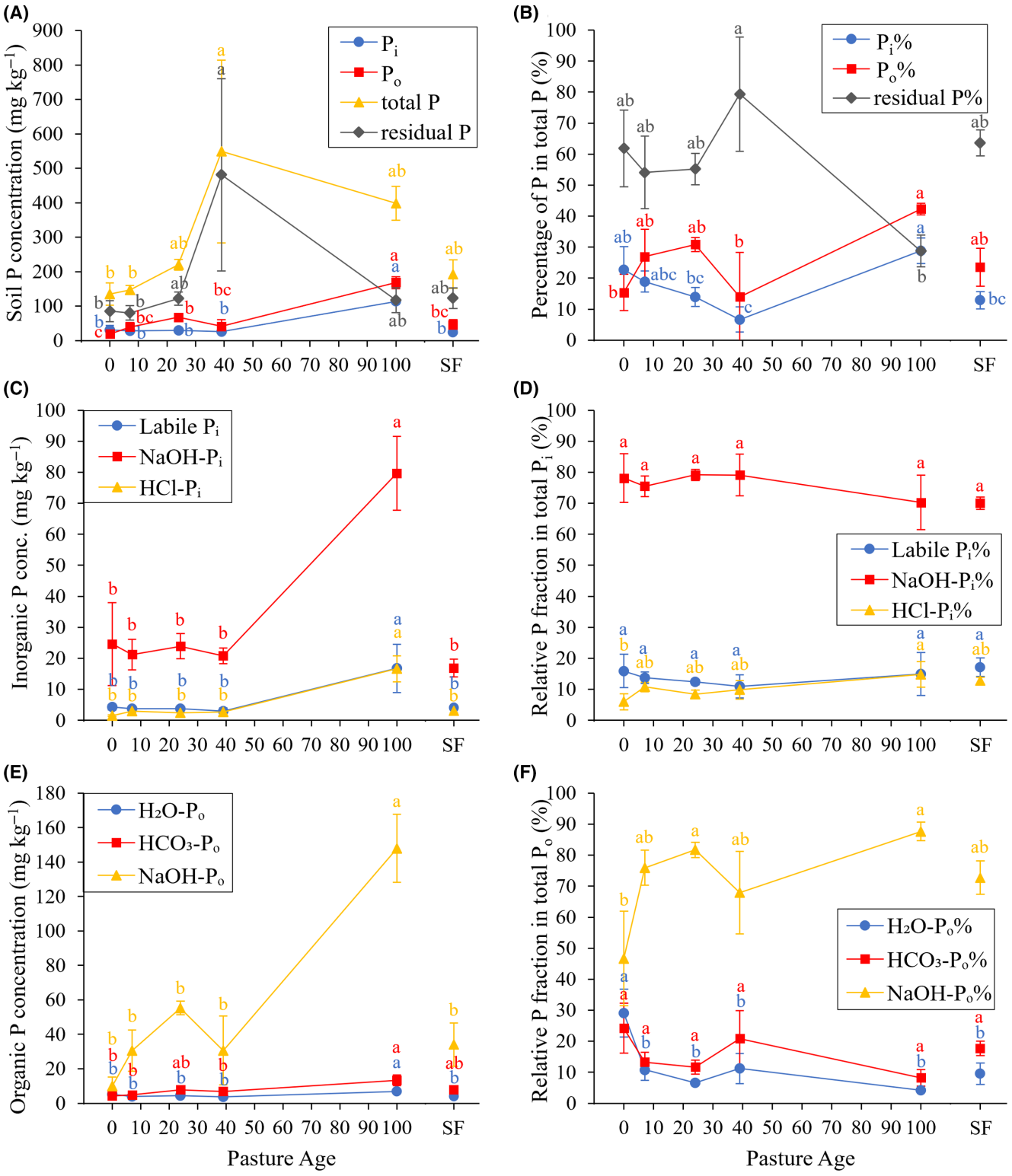

FIGURE 3 Concentration and proportion of soil total P and P fractions. (A) Concentrations (mg kg^{-1}) and (B) proportions (%) of total P, total inorganic P (P_i), total organic P (P_o), and residual P; (C) pool sizes (mg kg^{-1}) interpreted from sequentially extracted fractions and (D) relative proportions (%) of labile P_i, sodium hydroxide extractable P_i (NaOH-Pi), and hydrochloric acid extractable P_i (HCl-P_i) fractions in total P_i; (E) pool sizes (mg kg^{-1}), and (F) relative proportions (%) of water extractable P_o (H_2O-P_o), bicarbonate extractable P_o (HCO_3-P_o), and sodium hydroxide extractable P_o (NaOH-P_o) fractions in total P_o, of soils (0–10 cm depth) across a 100-year deforestation chronosequence in the Brazilian Amazon, in which primary forests (0 year) were converted to pasture. Soil P fractions were measured by modified Hedley sequential extraction. Also included is a 13-year-old secondary forest (SF) site established by reforestation of abandoned pasture. The standard deviations were calculated from $n = 3$ sites, indicating the within-site variations of each fraction. Different letters among pasture age indicate significant differences (Tukey's HSD, $p < .05$).

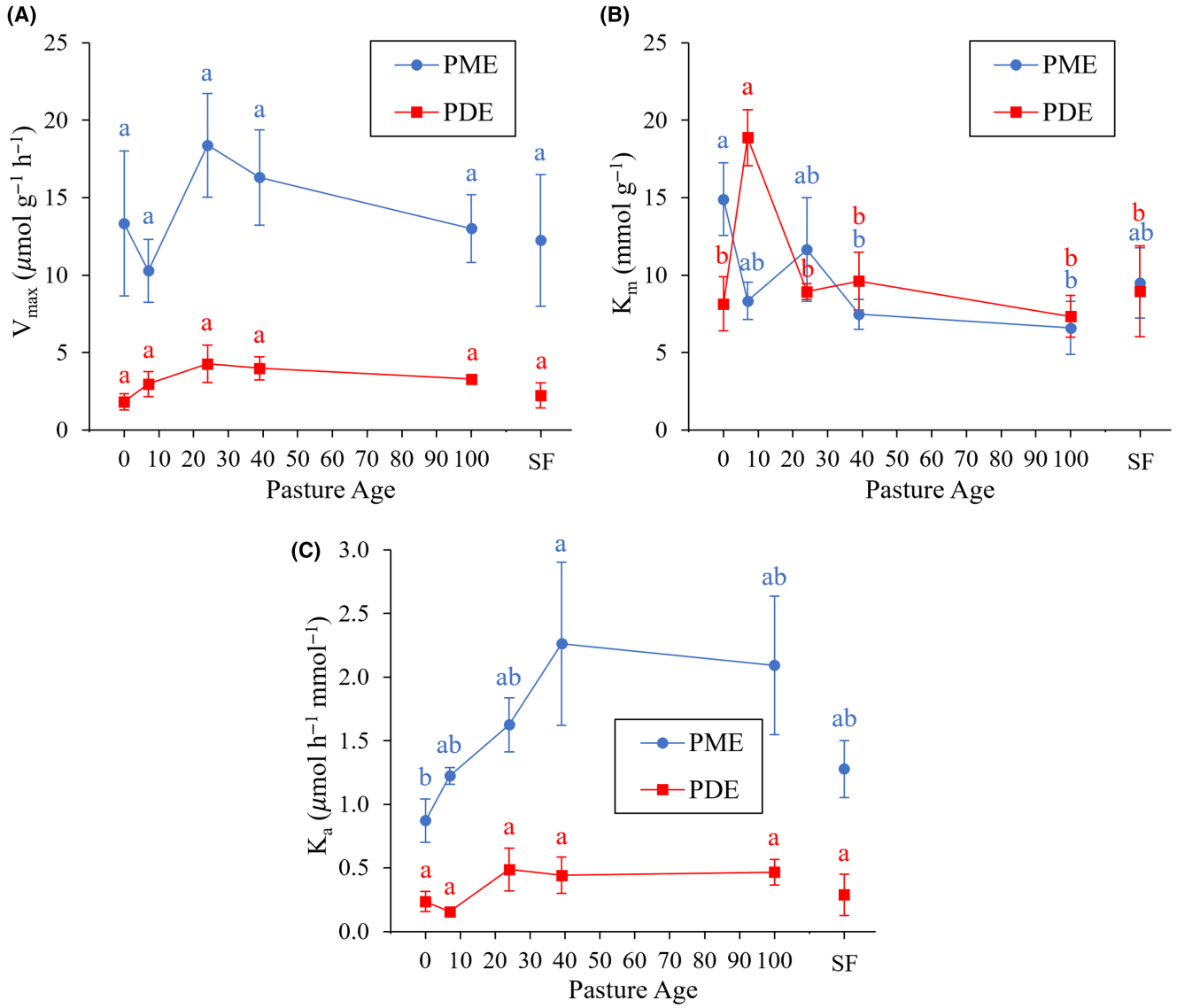

FIGURE 4 Fitted Michaelis–Menten kinetics model parameters (A) V_{max} (μmol pNP g^{-1} h^{-1}), (B) K_m (mmol g^{-1}), and (C) K_a (μmol pNP h^{-1} mmol^{-1}) of phosphomonoesterase (PME) and phosphodiesterase (PDE) in soils (0–10 cm depth) across a 100-year deforestation chronosequence in the Brazilian Amazon, in which primary forests (0 year) were converted to pasture. Also included is a 13-year-old secondary forest (SF) site established by reforestation of abandoned pasture. The standard deviations were calculated from $n = 3$ sites, indicating the within-site variations. Different letters among pasture age indicate significant differences (Tukey's HSD, $p < .05$).

However, we did not observe changes in labile P_i, which would be expected from pyromineralization and/or manure and urine deposition, until the transition from medium age (39y) to old (100y) pastures. The initial absence of change in labile P_i could be ascribed to the low transport of P during burning and subsequent fixation in soils. Up to 55% of the biomass P stock can be lost to the atmosphere in smoke depending on the slash-and-burn fire intensity (Kauffman et al., 1993; Raison et al., 1985; Romanya et al., 1994). The subsequent fixation of biomass ash P deposited on the soil surface with soil iron and aluminum minerals may further transform labile P to recalcitrant forms over time. As a result, increases in labile P in surface soils can be an order of magnitude lower than expected based on P stock in the burned aboveground biomass (Juo & Manu, 1996; Sanchez, 1977). The subsequent P inputs to surface soils via pasture grass biomass burning were likely of relatively low magnitude due to the low pasture grass aboveground biomass P content (~1–2 kg ha^{-1}) reported for pastures in the Amazon basin (Freitas et al., 2022). Post-burning increases in soil total P have been reported to be 10%, corresponding to approximately 8–11 kg ha^{-1} from the primary forests aboveground biomass P estimated to be ~56–63 kg ha^{-1}, with major losses (22–35 kg ha^{-1}) via ash blowing or smoke particulates (Kauffman et al., 1995). Our finding that labile P_i did not change in the first 39 years of pasture is consistent with other deforestation chronosequence studies in the Amazon limited to 15–40 year pastures (Asner et al., 2004; Garcia-Montiel et al., 2000). The increase in labile P_i after 39 years could be attributed to enhanced soil P mobility in the rhizosphere of *Brachiaria* (Merlin et al., 2015).

The XANES speciations of soil P were broadly consistent with pools inferred by sequential fractionation (Figures 2 and 3; Figure S3). For example, NaOH-P_i and HCl-P_i fractions were comparable to (Fe+Al)-P and Ca-P species via XANES, as expected (Maranguit et al., 2017), and the sum of all P_o fractions was comparable to the P_o pool via XANES. Our XANES results suggested that P_i in soils along the pasture age was dominated by (Fe+Al)-P (39%–53%), whereas Ca-P only covered a small portion (13%–15%) (Figure 2), which was consistent with the dominance of NaOH-P_i (25%–50% of total extractable P) followed by HCl-P_i (3%–6% of total extractable P) in P_i fractions from sequential extraction (Figure S3). This supports our interpretation of the NaOH-P_i and HCl-P_i fractions as operationally defined (Fe+Al)-P and Ca-P. Discrepancies between XANES and sequential extraction results can be ascribed to the over- or underestimated (Fe+Al)-P and Ca-P via extraction (Barrow & Debnath, 2020; Gu & Margenot, 2021) and the poor resolution of P_o by XANES (Prietzel et al., 2016). The proportion of P_o from XANES (37%–49%) was lower than P_o in total extractable P from Hedley fractionation (40%–69%), which can potentially lead to the greater relative speciation for (Fe+Al)-P and Ca-P.

The change of (Fe+Al)-P and Ca-P, generally considered recalcitrant pools (Negassa & Leinweber, 2009), with deforestation was similar to that of labile P_i. With periodic burning, a large amount of Ca can be deposited onto the soil via ash, which can increase the Ca-P pool (Chavarro-Bermeo et al., 2022; Garcia-Montiel et al., 2000; Juo & Manu, 1996). However, the acidic soil pH in the study area would lead to the dissolution of Ca-P precipitates. Our finding that (Fe+Al)-P was constant during the initial 39 years of deforestation is similar to others (Chavarro-Bermeo et al., 2022; Garcia-Montiel et al., 2000), and consistent with P_{ox} and P_{di} pools (Figure 1A,B) that provide an independent measure of P associated with iron and/or aluminum minerals. The decrease in the soil weathering degree index $Fe_{di}/(Fe_{ox}+Fe_{di})$ ratio with pasture age would appear to suggest a shift from a highly crystalline structure to poorly crystalline or amorphous following post-burn deforestation. The mineralogy of highly weathered soils is generally near-equilibrium and thus stable, the observed changes in fractions may not accurately reflect actual changes in situ. The lower $Fe_{di}/(Fe_{ox}+Fe_{di})$ ratio—indicative of greater P adsorption capacity (Zheng et al., 2012)—is also consistent with the increase in (Fe+Al)-P fraction (Figure 3C). Collectively, this suggests that the distribution of soil P across inorganic pools inferred by fractionation and XANES is relatively agnostic to land use change, with P_i pools changing in lockstep with net P accumulation in surface soils with pasture age.

4.2 | Soil P_o pools and deforestation

In contrast to soil P_i pools, soil total P_o continually increased with pasture age across a century, consistent with shorter-term (<50 years) evaluations (Garcia-Montiel et al., 2000; Hamer et al., 2013). Increases in total P_o with pasture age could be explained by (1) more rapid cycling of P_o in pasture ecosystems (Garcia-Montiel et al., 2000); (2) the decomposition of finer grassroots; and (3) a positive correlation between SOC and soil P_o (Hamer et al., 2013; Walker & Adams, 1958). Increased soil P_o under pasture hypothesized by Garcia-Montiel et al. (2000) to result from pasture species accessing residual P are supported by our results as an increase in soil P_o and a decline in residual P, especially in older (39–100y) pastures. At our site, pasture establishment is thought to have increased the fine-root density in surface soil, increasing SOC concentrations via direct addition of root-derived C (Durrer et al., 2021). *Brachiaria* roots could also directly add to the P_o fraction, which depending on the soil P content, may entail P concentrations from 0.07 to 2.71 g kg^{-1} (Merlin et al., 2015).

The increasing trend of NaOH-P_o% and the decreasing trend of labile P_o% (especially H_2O-P_o) with pasture age indicated that the increased total soil P_o disproportionally increases the non-labile compared to the labile P_o pool. After the forest-to-pasture conversion, *Brachiaria*-derived soil organic matter and to a lesser extent cattle excrement are the primary internal (i.e., not external or net) inputs of P_o to surface soils (0–10 cm depth). Furthermore, the release of labile P_o from root-derived organic matter or cattle excrement in forms such as phytate, one of the dominant P_o forms in highly weathered soils (McDowell & Stewart, 2006), is readily fixed by iron and aluminum minerals and thus would be extractable in the non-labile P_o fraction (Xu & Arai, 2022a, 2022b). The microbial biomass P was not measured in this study as it was identified as a minor P pool in weathered soils (~2–5 mg kg^{-1}) (Moreira et al., 2011; Moreira & Fageria, 2011).

The soil C:P_o ratio has been proposed to determine whether soil is P limiting to microbial biomass, analogous to the mineralization–immobilization thresholds developed for soil C:N (Arenberg & Arai, 2019). Soils with sufficient available P were hypothesized to have a C:P_o < 100, whereas the C:P_o > 200 indicates relative P limitation (Dieter et al., 2010; Maranguit et al., 2017). With high soil available P concentrations, P_o mineralization catalyzed by phosphatases is generally thought to be attenuated, which might result in a net increase in P_o and a reduced C:P_o ratio (Dieter et al., 2010; Zhao et al., 2008). On the other hand, under low P availability, phosphatase secretion and thus extracellular activity increases (Spohn & Kuzyakov, 2013), potentially elevating the C:P_o ratio (Dieter et al., 2010; Mcgill & Cole, 1981). We only observed a C:P_o < 200 in the centennial pasture, suggesting that forests and younger pastures may have had aggravated P limitation (Maranguit et al., 2017). The reduced C:P_o in the oldest pasture was due to the magnitude of total P_o increase (from 19.3 to 168 mg kg^{-1}) exceeding SOC increase (from 7.9 to 23.4 g kg^{-1}) with long-term pasture age.

4.3 | The response of phosphatase on deforestation

Differences in V_{max} and K_m of soil PME and PDE by land use and duration reflect shifts in isozymes produced by distinct microbial and plant species that collectively constitute the total pool of activity

(Williams, 1973), and may also reflect differences in substrate availability (P_o) and product concentration (labile P_i). Higher substrate concentrations can stimulate enzyme production by plant roots and soil microorganisms and can favor the production of enzymes with higher V_{max} (Sinsabaugh & Shah, 2010, 2012; Stone & Plante, 2014). Meanwhile, the elevated concentration of product can inhibit enzyme activity (i.e., feedback inhibition), potentially leading to a lower apparent V_{max} (Sinsabaugh & Shah, 2010). The lack of change in V_{max} of both PME and PDE across a century of pastures is consistent with relatively stable soil P_o (i.e., substrate) and labile P_i (i.e., product) during the initial 39 years of pasture, and the proportional increase in both fractions from 39 to 100 years, which potentially lead to the counterbalanced substrate stimulation and feedback inhibition on apparent V_{max}.

The enzyme-substrate binding affinity K_m can be used to describe relative substrate availability in soils (Sinsabaugh & Shah, 2010). Although not inherently related, V_{max} and K_m are often positively associated (Sinsabaugh & Shah, 2012; Williams, 1973), including soil PME (Hui et al., 2013). We did not observe a positive correlation between V_{max} and K_m, as K_m generally decreased with pasture age for both PME and PDE—opposite to the soil P_o change. An opposite trend between K_m and the substrate P_o was expected since lower K_m values signify higher substrate affinities. Forest-to-pasture conversion at our site entailed shifts in soil microbial community structure (Paula et al., 2014; Rodrigues et al., 2013), which may have altered isoenzyme composition and thus kinetic properties of the soil extracellular enzyme pool (Farrell et al., 1994; Khalili et al., 2011; Tabatabai et al., 2002). The K_a normalizes the V_{max} to K_m as a metric of catalytic efficiency (Esti et al., 2011; Li & Margenot, 2021; Stone & Plante, 2014). Increases in K_a of both PME and PDE with pasture age suggested that in older pastures, the microbial–plant consortium shifted to the production of phosphates with greater catalytic efficiency than in younger pastures or primary forests.

4.4 | Soil P cycling in the secondary forests

Soil P pool sizes and enzyme-proxied cycling rates were similar between primary and secondary forests, supporting our hypothesis that soil P cycling variables after reforestation would revert to similar pool sizes or rates as in primary forests within 13 years. In our study site, the secondary forest was developed by natural recolonization on pastures abandoned after 7–10 years of grazing, which is typical of the region (Aguiar et al., 2016; Durrer et al., 2021). It is possible that the duration of pasture before abandonment and secondary forest establishment at our site may have been insufficiently long to detect initial deforestation effects on soil P cycling: P pool sizes in the youngest pasture (7y) were also similar to both primary and secondary forests. When comparing secondary forests to medium-age pastures (17–50 years), similar to our results, decreases in P fractions were reported in secondary forests abandoned for 10 years with the only exception for labile P, which showed no change (Hamer et al., 2013). Similarly, no difference in P pools between primary and secondary forests abandoned for 10 years was found by Hamer et al. (2013), though the pre-abandonment pasture duration was not reported. Without knowing pre-abandonment pasture duration, it is difficult to compare secondary forests with pastures. However, since soil P pools in secondary forests are not usually evaluated, our comparison provides an initial benchmark evaluation of how soil P may differ between the secondary forest and pastures. General decreases in total soil P in early reforestation (~20 years) after pasture abandonment likely reflect immobilization in forest vegetation biomass (Hamer et al., 2013; McGrath et al., 2001).

Despite the reversion of soil P cycling indicators, the growth of secondary forests after pasture abandonment is also generally P limited as the remaining soil P supply may constrain forest regrowth (Lawrence & Schlesinger, 2001), especially with zero fertilizer inputs of P during pasture management. However, the P limitation status should not be exaggerated by pasture use after deforestation, as soil P output by cattle removal was relatively minimal (Buschbacher, 1987), and we observed increases in soil P pools at 0–10 cm depth with pasture age, including labile P_i. Reversion of P pool sizes and process rates in 13-year-old secondary forest also suggests the potential of reforestation without the need for P fertilization, which has been proposed by some (Ganade & Brown, 2002; Markewitz et al., 2012). Furthermore, we acknowledge that our study was limited to evaluating only surface soils, whereas other studies have found a similar or even higher subsoil P content compared to surface soils in both primary forests and pastures in the Amazon basin (Chavarro-Bermeo et al., 2022; Garcia-Montiel et al., 2000). Increases in surface soil P pools and total P with pasture age is likely due to biological pumping of P (i.e., deep-rooted grass acquires P from subsoil and then grass residue deposit on surface soil), which could lead to lower subsoil P in the long term. Subsoil P should also be addressed in future evaluations of P cycling in converted pastures and secondary forests to provide insights to pasture sustainability and forest restoration in this region of the Amazon.

The use of observational chronosequence might overlook the potential differences in the initial soil P reservoir across our study site. The atmospheric P deposition input to the Amazon basin from Saharan dust (e.g., up to ~0.005–0.16 kg P ha^{-1} $year^{-1}$) (Kok et al., 2021; Mahowald et al., 2005; Wang et al., 2023), which is representative of the Amazon basin, can potentially shift the initial total P content of surface soil with different years of P deposition before pasture establishment. However, with relatively small input (cumulatively ~0.5–16 kg P ha^{-1} for 100 years) and the potentially similar P composition as soil P, which can be dominated by Fe/Al-P (44%–73%) due to atmospheric acidification during dust transport (Dam et al., 2021), atmospheric P input is expected to cause only minor differences in soil P content and forms, and should not change the overall trend of soil P cycling with deforestation and reforestation. Another possible source of difference is the growth of primary forest with time, which can cause differences in soil P and aboveground biomass P contents in primary forests before conversion. However, changes in vegetation stored P in primary forests over 100 years might not be evident, as the increase in total aboveground biomass C

within 10 years in Brazil was found to be minor (Fawcett et al., 2022), and thus, the impacts on changes in soil P with pasture age are also expected to be minor. With the potential sources of differences, it is worth noting that differences in the initial P pool sizes and rates might also account for the observed variability (i.e., total P in 39y pasture) and lack of change in soil P pools. Moreover, the comparisons of the proportion of P pools would alleviate the impacts of difference in initial total P concentrations and provide us with the trends of the P pools with deforestation.

More broadly, our results underscore the need for experimental evaluations of deforestation and reforestation effects on soil P cycling at temporal scales of multiple decades. Empirical assessments of soil P and thus secondary forests P limitation are rarely evaluated at the appropriate timescales: modeling indicates that changes in soil P with deforestation and reforestation can require decades to a century to equilibrate (Nagy et al., 2017). Future meta-analysis on soil P response to deforestation and reforestation would also be needed once additional research studies (such as ours) are performed. Finally, both the pasture duration history and the secondary forest age should be considered when investigating reforestation chronosequences. Missing information on pasture age prior to abandonment and the lack of long-term reforestation (e.g., >20 years) complicate interpretation of soil P cycling under secondary forests, as in our and many other studies utilizing observational chronosequences. Evaluating P pool dynamics throughout the soil profile under both deforestation and reforestation at a long-term (centennial) scale would enable model calibration to predict P cycling and potential P limitations to agricultural and non-managed agroecosystems in the Amazon basin.

5 | CONCLUSION

This study revealed that the conversion of Amazon primary forests to pastures entails increases in surface soil P pool sizes over a century, but that soil P cycling can revert to values similar to those of primary forests within two decades with forest regrowth by natural succession from nearby intact primary forests. In surface soils, P pool sizes increased in centennial pastures relative to primary forest, suggesting that the increase in total soil P concomitantly increased P pools. This likely reflected surface deposition of aboveground biomass P by pasture grasses, enhanced by periodic burning and with negligible P export by low-density grazing. Soil phosphatase V_{max} did not respond to deforestation, but K_m decreased and K_a increased with pasture age. Soil P variables and phosphatase catalysis parameters were similar between primary and secondary forests (13 years), indicating that soil P cycling with natural succession forest regrowth might be able to revert to similar pool sizes or rates observed in primary forests within less than two decades.

AUTHOR CONTRIBUTIONS

Suwei Xu: Formal analysis; visualization; writing – original draft; writing – review and editing. **Chunhao Gu:** Investigation; writing – review and editing. **Jorge L. M. Rodrigues:** Conceptualization; funding acquisition; methodology; writing – review and editing. **Chongyang Li:** Investigation; writing – review and editing. **Brendan Bohannan:** Methodology; resources; writing – review and editing. **Klaus Nüsslein:** Methodology; resources; writing – review and editing. **Andrew J. Margenot:** Conceptualization; data curation; funding acquisition; investigation; supervision; writing – review and editing.

ACKNOWLEDGMENTS

The authors thank the owners and staff of Agropecuaria Nova Vida for logistic support and permission to work on their property. We are grateful to Dr. S.M. Tsai and Wagner Picinini for their assistance with sampling. This project was supported in part by the Agriculture and Food Research Initiative Competitive Grant (2009-35319-05186) from the US Department of Agriculture—National Institute of Food and Agriculture (NIFA). The authors are grateful to the beamline scientists Yongfeng Hu and Qunfeng Xiao at the Canadian Light Source for providing technical support for P K-edge XANES data collection. A portion of the research described in this work was conducted at the Canadian Light Source, a national research facility of the University of Saskatchewan, which is supported by the Canada Foundation for Innovation (CFI), the Natural Sciences and Engineering Research Council (NSERC), the National Research Council (NRC), the Canadian Institutes of Health Research (CIHR), and the Government of Saskatchewan, and the University of Saskatchewan.

CONFLICT OF INTEREST STATEMENT

The authors declare no competing interests.

DATA AVAILABILITY STATEMENT

The data that support the findings of this study are openly available in Dryad at https://datadryad.org/stash/share/ClvSYvW1R7M6NiwXQ3U6EgfE9RIOWWkW566YnfcZOY4.

ORCID

Suwei Xu https://orcid.org/0000-0002-9501-8902

Andrew J. Margenot https://orcid.org/0000-0003-0185-8650

REFERENCES

Aguiar, A. P. D., Vieira, I. C. G., Assis, T. O., Dalla-Nora, E. L., Toledo, P. M., Santos-Junior, R. A. O., Batistella, M., Coelho, A. S., Savaget, E. K., Aragão, L. E., Nobre, C. A., & Ometto, J. P. H. (2016). Land use change emission scenarios: Anticipating a forest transition process in the Brazilian Amazon. *Global Change Biology*, *22*(5), 1821–1840. https://doi.org/10.1111/gcb.13134

Arenberg, M. R., & Arai, Y. (2019). Uncertainties in soil physicochemical factors controlling phosphorus mineralization and immobilization processes. *Advances in Agronomy*, *154*(154), 153–200. https://doi.org/10.1016/bs.agron.2018.11.005

Arenberg, M. R., & Arai, Y. (2021). Effects of native leaf litter amendments on phosphorus mineralization in temperate floodplain soils. *Chemosphere*, *266*, 129210. https://doi.org/10.1016/j.chemosphere.2020.129210

Asner, G. P., Townsend, A. R., Bustamante, M. M. C., Nardoto, G. B., & Olander, L. P. (2004). Pasture degradation in the central Amazon: Linking changes in carbon and nutrient cycling with remote sensing.

Global Change Biology, *10*(5), 844–862. https://doi.org/10.1111/j.1529-8817.2003.00766.x

Barrow, N. J., & Debnath, A. (2020). Reply to: Navigating limitations and opportunities of soil phosphorus fractionation: A comment on "The soil phosphate fractionation fallacy" by Barrow et al. 2020. *Plant and Soil*, *453*(1–2), 595–596. https://doi.org/10.1007/s11104-020-04574-5

Bastos, T. X., & Diniz, T. D. (1982). *Avaliação do Clima do Estado de Rondônia Para Desenvolvimento Agrícola*. Embrapa-CPATU.

Brown, J. C., Jepson, W., & Price, K. P. (2004). Expansion of mechanized agriculture and land-cover change in southern Rondônia, Brazil. *Journal of Latin American Geography*, *3*(2), 96–102.

Brown, S., & Lugo, A. E. (1990). Tropical secondary forests. *Journal of Tropical Ecology*, *6*, 1–32. https://doi.org/10.1017/S0266467400003989

Buschbacher, R. J. (1987). Cattle productivity and nutrient fluxes on an Amazon pasture. *Biotropica*, *19*(3), 200–207. https://doi.org/10.2307/2388337

Butt, N., de Oliveira, P. A., & Costa, M. H. (2011). Evidence that deforestation affects the onset of the rainy season in Rondonia, Brazil. *Journal of Geophysical Research-Atmospheres*, *116*, D11120. https://doi.org/10.1029/2010jd015174

Cerri, C. E. P., Paustian, K., Bernoux, M., Victoria, R. L., Melillo, J. M., & Cerri, C. C. (2004). Modeling changes in soil organic matter in Amazon forest to pasture conversion with the century model. *Global Change Biology*, *10*(5), 815–832. https://doi.org/10.1111/j.1365-2486.2004.00759.x

Cervelli, S., Nannipieri, P., Ceccanti, B., & Sequi, P. (1973). Michaelis constant of soil acid phosphatase. *Soil Biology and Biochemistry*, *5*(6), 841–845. https://doi.org/10.1016/0038-0717(73)90029-1

Chavarro-Bermeo, J. P., Arruda, B., Mora-Motta, D. A., Bejarano-Herrera, W., Ortiz-Morea, F. A., Somenahally, A., & Silva-Olaya, A. M. (2022). Responses of soil phosphorus fractions to land-use change in Colombian Amazon. *Sustainability*, *14*, 2285. https://doi.org/10.3390/su14042285

Cunha, H. F. V., Andersen, K. M., Lugli, L. F., Santana, F. D., Aleixo, I. F., Moraes, A. M., Garcia, S., di Ponzio, R., Mendoza, E. O., Brum, B., Rosa, J. S., Cordeiro, A. L., Portela, B. T. T., Ribeiro, G., Coelho, S. D., de Souza, S. T., Silva, L. S., Antonieto, F., Pires, M., … Quesada, C. A. (2022). Direct evidence for phosphorus limitation on Amazon forest productivity. *Nature*, *608*(7923), 558–562. https://doi.org/10.1038/s41586-022-05085-2

Dalling, J. W., Heineman, K., Lopez, O. R., Wright, S. J., & Turner, B. L. (2016). Nutrient availability in tropical rain forests: The paradigm of phosphorus limitation. In G. Goldstein & L. S. Santiago (Eds.), *Tropical tree physiology* (pp. 261–273). Springer.

Dam, T. T. N., Angert, A., Krom, M. D., Bigio, L., Hu, Y. F., Beyer, K. A., Mayol-Bracero, O. L., Santos-Figueroa, G., Pio, C., & Zhu, M. Q. (2021). X-ray spectroscopic quantification of phosphorus transformation in Saharan dust during trans-Atlantic dust transport. *Environmental Science & Technology*, *55*(18), 12694–12703. https://doi.org/10.1021/acs.est.1c01573

Damgaard, C. (2019). A critique of the space-for-time substitution practice in community ecology. *Trends in Ecology & Evolution*, *34*(5), 416–421. https://doi.org/10.1016/j.tree.2019.01.013

Danielson, R. E., & Rodrigues, J. L. M. (2022). Impacts of land-use change on soil microbial communities and their function in the Amazon rainforest. *Advances in Agronomy*, *175*(175), 179–258. https://doi.org/10.1016/bs.agron.2022.04.001

De Palma, A., Sanchez-Ortiz, K., Martin, P. A., Chadwick, A., Gilbert, G., Bates, A. E., Börger, L., Contu, S., Hill, S. L., & Purvis, A. (2018). Chapter four—Challenges with inferring how land-use affects terrestrial biodiversity: Study design, time, space and synthesis. In D. A. Bohan, A. J. Dumbrell, G. Woodward, & M. Jackson (Eds.), *Advances in ecological research* (Vol. *58*, pp. 163–199). Academic Press.

Dieter, D., Elsenbeer, H., & Turner, B. L. (2010). Phosphorus fractionation in lowland tropical rainforest soils in central Panama. *Catena*, *82*(2), 118–125. https://doi.org/10.1016/j.catena.2010.05.010

Durrer, A., Margenot, A. J., Silva, L. C. R., Bohannan, B. J. M., Nusslein, K., van Haren, J., Andreote, F. D., Parikh, S. J., & Rodrigues, J. L. M. (2021). Beyond total carbon: Conversion of amazon forest to pasture alters indicators of soil C cycling. *Biogeochemistry*, *152*(2–3), 179–194. https://doi.org/10.1007/s10533-020-00743-x

Esti, M., Benucci, I., Liburdi, K., & Garzillo, A. M. V. (2011). Effect of wine inhibitors on free pineapple stem bromelain activity in a model wine system. *Journal of Agricultural and Food Chemistry*, *59*(7), 3391–3397. https://doi.org/10.1021/jf104919v

Farrell, R. E., Gupta, V. V. S. R., & Germida, J. J. (1994). Effects of cultivation on the activity and kinetics of arylsulfatase in Saskatchewan soils. *Soil Biology & Biochemistry*, *26*(8), 1033–1040. https://doi.org/10.1016/0038-0717(94)90118-X

Fawcett, D., Sitch, S., Ciais, P., Wigneron, J. P., Silva-Junior, C. H. L., Heinrich, V., Vancutsem, C., Achard, F., Bastos, A., Yang, H., Li, X., Albergel, C., Friedlingstein, P., & Aragão, L. E. O. C. (2022). Declining Amazon biomass due to deforestation and subsequent degradation losses exceeding gains. *Global Change Biology*, *29*, 1106–1118. https://doi.org/10.1111/gcb.16513

Feigl, B., Cerri, C., Piccolo, M., Noronha, N., Augusti, K., Melillo, J., Eschenbrenner, V., & Melo, L. (2006). Biological survey of a low-productivity pasture in Rondônia state, Brazil. *Outlook on Agriculture*, *35*(3), 199–208. https://doi.org/10.5367/000000006778536738

Freitas, R. G., Pereira, F. R. S., Dos Reis, A. A., Magalha, P. S. G., Figueiredo, G. K. D. A., & Do Amaral, L. R. (2022). Estimating pasture aboveground biomass under an integrated crop-livestock system based on spectral and texture measures derived from UAV images. *Computers and Electronics in Agriculture*, *198*, 107122. https://doi.org/10.1016/j.compag.2022.107122

Friesen, D. K., Rao, I. M., Thomas, R. J., Oberson, A., & Sanz, J. I. (1997). Phosphorus acquisition and cycling in crop and pasture systems in low fertility tropical soils. *Plant and Soil*, *196*(2), 289–294. https://doi.org/10.1023/A:1004226708485

Ganade, G., & Brown, V. K. (2002). Succession in old pastures of central Amazonia: Role of soil fertility and plant litter. *Ecology*, *83*(3), 743–754. https://doi.org/10.1890/0012-9658(2002)083[0743:Siopoc]2.0.Co;2

Garcia-Montiel, D. C., Neill, C., Melillo, J., Thomas, S., Steudler, P. A., & Cerri, C. C. (2000). Soil phosphorus transformations following forest clearing for pasture in the Brazilian Amazon. *Soil Science Society of America Journal*, *64*(5), 1792–1804. https://doi.org/10.2136/sssaj2000.6451792x

German, D. P., Weintraub, M. N., Grandy, A. S., Lauber, C. L., Rinkes, Z. L., & Allison, S. D. (2011). Optimization of hydrolytic and oxidative enzyme methods for ecosystem studies. *Soil Biology and Biochemistry*, *43*(7), 1387–1397. https://doi.org/10.1016/j.soilbio.2011.03.017

Gu, C., Dam, T., Hart, S. C., Turner, B. L., Chadwick, O. A., Berhe, A. A., Hu, Y., & Zhu, M. (2020). Quantifying uncertainties in sequential chemical extraction of soil phosphorus using XANES spectroscopy. *Environmental Science & Technology*, *54*, 2257–2267. https://doi.org/10.1021/acs.est.9b05278

Gu, C., Hart, S. C., Turner, B. L., Hu, Y., Meng, Y., & Zhu, M. (2019). Aeolian dust deposition and the perturbation of phosphorus transformations during long-term ecosystem development in a cool, semi-arid environment. *Geochimica et Cosmochimica Acta*, *246*, 498–514.

Gu, C. H., & Margenot, A. J. (2021). Navigating limitations and opportunities of soil phosphorus fractionation. *Plant and Soil*, *459*(1–2), 13–17. https://doi.org/10.1007/s11104-020-04552-x

Hamer, U., Potthast, K., Burneo, J. I., & Makeschin, F. (2013). Nutrient stocks and phosphorus fractions in mountain soils of Southern Ecuador after conversion of forest to pasture. *Biogeochemistry*, *112*(1–3), 495–510. https://doi.org/10.1007/s10533-012-9742-z

Han, E. S., Li, F., Perkons, U., Küpper, P. M., Bauke, S. L., Athmann, M., Thorup-Kristensen, K., Kautz, T., & Köpke, U. (2021). Can precrops uplift subsoil nutrients to topsoil? *Plant and Soil*, *463*(1–2), 329–345. https://doi.org/10.1007/s11104-021-04910-3

Hedley, M., Stewart, J., & Chauhan, B. (1982). Changes in inorganic and organic soil phosphorus fractions induced by cultivation practices and by laboratory incubations. *Soil Science Society of America Journal*, *46*(5), 970–976.

Hui, D. F., Mayes, M. A., & Wang, G. S. (2013). Kinetic parameters of phosphatase: A quantitative synthesis. *Soil Biology & Biochemistry*, *65*, 105–113. https://doi.org/10.1016/j.soilbio.2013.05.017

INPE. (2011). *Program for the estimation of Amazon deforestation (Projeto PRODES digital)*. Brazilian National Institute for Space Research. http://www.dpi.inpe.br/prodesdigital/prodes.php

Juo, A. S. R., & Manu, A. (1996). Chemical dynamics in slash-and-burn agriculture. *Agriculture Ecosystems & Environment*, *58*(1), 49–60. https://doi.org/10.1016/0167-8809(95)00656-7

Kauffman, J. B., Cummings, D. L., Ward, D. E., & Babbitt, R. (1995). Fire in the Brazilian Amazon. 1. Biomass, nutrient pools, and losses in slashed primary forests. *Oecologia*, *104*(4), 397–408. https://doi.org/10.1007/Bf00341336

Kauffman, J. B., Sanford, R. L., Cummings, D. L., Salcedo, I. H., & Sampaio, E. V. S. B. (1993). Biomass and nutrient dynamics associated with slash fires in neotropical dry forests. *Ecology*, *74*(1), 140–151. https://doi.org/10.2307/1939509

Kettler, T. A., Doran, J. W., & Gilbert, T. L. (2001). Simplified method for soil particle-size determination to accompany soil-quality analyses. *Soil Science Society of America Journal*, *65*(3), 849–852. https://doi.org/10.2136/sssaj2001.653849x

Khalili, B., Nourbakhsh, F., Nili, N., Khademi, H., & Sharifnabi, B. (2011). Diversity of soil cellulase isoenzymes is associated with soil cellulase kinetic and thermodynamic parameters. *Soil Biology & Biochemistry*, *43*(8), 1639–1648. https://doi.org/10.1016/j.soilbio.2011.03.019

Kok, J. F., Adebiyi, A. A., Albani, S., Balkanski, Y., Checa-Garcia, R., Chin, M. A., Colarco, P. R., Hamilton, D. S., Huang, Y., Ito, A., Klose, M., Li, L., Mahowald, N. M., Miller, R. L., Obiso, V., García-Pando, C. P., Rocha-Lima, A., & Wan, J. S. (2021). Contribution of the world's main dust source regions to the global cycle of desert dust. *Atmospheric Chemistry and Physics*, *21*(10), 8169–8193. https://doi.org/10.5194/acp-21-8169-2021

Lawrence, D., & Schlesinger, W. H. (2001). Changes in soil phosphorus during 200 years of shifting cultivation in Indonesia. *Ecology*, *82*(10), 2769–2780. https://doi.org/10.2307/2679959

Leite, C. C., Costa, M. H., de Lima, C. A., Ribeiro, C. A., & Sediyama, G. C. (2011). Historical reconstruction of land use in the Brazilian Amazon (1940–1995). *Journal of Land Use Science*, *6*(1), 33–52. https://doi.org/10.1080/1747423X.2010.501157

Li, C., & Margenot, A. J. (2021). Apparent kinetic properties of soil phosphomonoesterase and β-glucosidase are disparately influenced by pH. *Soil Science Society of America Journal*, *85*(6), 2007–2018. https://doi.org/10.1002/saj2.20332

Mahowald, N. M., Artaxo, P., Baker, A. R., Jickells, T. D., Okin, G. S., Randerson, J. T., & Townsend, A. R. (2005). Impacts of biomass burning emissions and land use change on Amazonian atmospheric phosphorus cycling and deposition. *Global Biogeochemical Cycles*, *19*(4), Gb4030. https://doi.org/10.1029/2005gb002541

Malhi, Y., Roberts, J. T., Betts, R. A., Killeen, T. J., Li, W. H., & Nobre, C. A. (2008). Climate change, deforestation, and the fate of the Amazon. *Science*, *319*(5860), 169–172. https://doi.org/10.1126/science.1146961

Malingreau, J. P., & Tucker, C. J. (1988). Large-scale deforestation in the southeastern Amazon Basin of Brazil. *Ambio*, *17*(1), 49–55.

Maranguit, D., Guillaume, T., & Kuzyakov, Y. (2017). Land-use change affects phosphorus fractions in highly weathered tropical soils. *Catena*, *149*, 385–393. https://doi.org/10.1016/j.catena.2016.10.010

Margenot, A. J., Nakayama, Y., & Parikh, S. J. (2018). Methodological recommendations for optimizing assays of enzyme activities in soil samples. *Soil Biology and Biochemistry*, *125*, 350–360.

Markewitz, D., Figueiredo, R. D., de Carvalho, C. J. R., & Davidson, E. A. (2012). Soil and tree response to P fertilization in a secondary tropical forest supported by an Oxisol. *Biology and Fertility of Soils*, *48*(6), 665–678. https://doi.org/10.1007/s00374-011-0659-9

McDowell, R. W., & Stewart, I. (2006). The phosphorus composition of contrasting soils in pastoral, native and forest management in Otago, New Zealand: Sequential extraction and P-31 NMR. *Geoderma*, *130*(1–2), 176–189. https://doi.org/10.1016/j.geoderma.2005.01.020

Mcgill, W. B., & Cole, C. V. (1981). Comparative aspects of cycling of organic C, N, S and P through soil organic-matter. *Geoderma*, *26*(4), 267–286. https://doi.org/10.1016/0016-7061(81)90024-0

McGrath, D. A., Smith, C. K., Gholz, H. L., & Oliveira, F. D. A. (2001). Effects of land-use change on soil nutrient dynamics in Amazônia. *Ecosystems*, *4*(7), 625–645. https://doi.org/10.1007/s10021-001-0033-0

Mehlich, A. (2008). Mehlich 3 soil test extractant: A modification of Mehlich 2 extractant. *Communications in Soil Science and Plant Analysis*, *15*(12), 1409–1416. https://doi.org/10.1080/00103628409367568

Merlin, A., Rosolem, C. A., & He, Z. (2015). Non-labile phosphorus acquisition by Brachiaria. *Journal of Plant Nutrition*, *39*(9), 1319–1327. https://doi.org/10.1080/01904167.2015.1109117

Miyanishi, K., & Johnson, E. A. (2007). 8—Coastal dune succession and the reality of dune processes. In E. A. Johnson & K. Miyanishi (Eds.), *Plant disturbance ecology* (pp. 249–282). Academic Press.

Moreira, A., & Fageria, N. K. (2011). Changes in soil properties under two different management systems in the western Amazon. *Communications in Soil Science and Plant Analysis*, *42*(21), 2666–2681. https://doi.org/10.1080/00103624.2011.614041

Moreira, A., Fageria, N. K., & Garcia, A. G. Y. (2011). Soil fertility, mineral nitrogen, and microbial biomass in upland soils of the central Amazon under different plant covers. *Communications in Soil Science and Plant Analysis*, *42*(6), 694–705. https://doi.org/10.1080/00103624.2011.550376

Murphy, J., & Riley, J. P. (1962). A modified single solution method for the determination of phosphate in natural waters. *Analytica Chimica Acta*, *27*, 31–36.

Nagy, R. C., Rastetter, E. B., Neill, C., & Porder, S. (2017). Nutrient limitation in tropical secondary forests following different management practices. *Ecological Applications*, *27*(3), 734–755. https://doi.org/10.1002/eap.1478

Nannipieri, P., Trasar-Cepeda, C., & Dick, R. P. (2017). Soil enzyme activity: A brief history and biochemistry as a basis for appropriate interpretations and meta-analysis. *Biology and Fertility of Soils*, *54*(1), 11–19. https://doi.org/10.1007/s00374-017-1245-6

Neal, J. L., Linkins, A. E., & Wallace, P. M. (1981). Influence of temperature on nonenzymatic hydrolysis of P-nitrophenyl phosphate in soil. *Communications in Soil Science and Plant Analysis*, *12*(3), 279–287. https://doi.org/10.1080/00103628109367149

Negassa, W., & Leinweber, P. (2009). How does the Hedley sequential phosphorus fractionation reflect impacts of land use and management on soil phosphorus: A review. *Journal of Plant Nutrition and Soil Science*, *172*(3), 305–325. https://doi.org/10.1002/jpln.200800223

Neill, C., Cerri, C. C., Melillo, J. M., Feigl, B. J., Moraes, J. F., & Piccolo, M. C. (1997). Stocks and dynamics of soil carbon following deforestation for pasture in Rondonia. In R. Lal, J. M. Kimble, R. F. Follett, & B. A. Stewart (Eds.), *Soil processes and the carbon cycle* (pp. 9–28). CRC Press.

Neill, C., Chaves, J. E., Biggs, T., Deegan, L. A., Elsenbeer, H., Figueiredo, R. O., Germer, S., Johnson, M. S., Lehmann, J., Markewitz, D., & Piccolo, M. C. (2011). Runoff sources and land cover change in the

Amazon: An end-member mixing analysis from small watersheds. *Biogeochemistry*, *105*(1–3), 7–18. https://doi.org/10.1007/s10533-011-9597-8

Neill, C., Deegan, L. A., Thomas, S. M., & Cerri, C. C. (2001). Deforestation for pasture alters nitrogen and phosphorus in small Amazonian streams. *Ecological Applications*, *11*(6), 1817–1828. https://doi.org/10.1890/1051-0761(2001)011[1817:Dfpana]2.0.Co;2

Neill, C., Melillo, J. M., Steudler, P. A., Cerri, C. C., de Moraes, J. F. L., Piccolo, M. C., & Brito, M. (1997). Soil carbon and nitrogen stocks following forest clearing for pasture in the southwestern Brazilian Amazon. *Ecological Applications*, *7*(4), 1216–1225.

Nogueira, E. M., Yanai, A. M., Fonseca, F. O. R., & Fearnside, P. M. (2015). Carbon stock loss from deforestation through 2013 in Brazilian Amazonia. *Global Change Biology*, *21*(3), 1271–1292. https://doi.org/10.1111/gcb.12798

Paula, F. S., Rodrigues, J. L. M., Zhou, J., Wu, L., Mueller, R. C., Mirza, B. S., Bohannan, B. J., Nüsslein, K., Deng, Y., Tiedje, J. M., & Pellizari, V. H. (2014). Land use change alters functional gene diversity, composition and abundance in Amazon forest soil microbial communities. *Molecular Ecology*, *23*(12), 2988–2999. https://doi.org/10.1111/mec.12786

Pedlowski, M. A., Dale, V. H., Matricardi, E. A. T., & da Silva, E. P. (1997). Patterns and impacts of deforestation in Rondonia, Brazil. *Landscape and Urban Planning*, *38*(3–4), 149–157. https://doi.org/10.1016/S0169-2046(97)00030-3

Pires, J. M., & Prance, G. T. (1985). The vegetation types of the Brazilian Amazon. In G. T. Prance & T. E. Lovejoy (Eds.), *Amazonia: Key environments* (pp. 109–145). Pergamon Press.

Prietzel, J., Klysubun, W., & Werner, F. (2016). Speciation of phosphorus in temperate zone forest soils as assessed by combined wet-chemical fractionation and XANES spectroscopy. *Journal of Plant Nutrition and Soil Science*, *179*(2), 168–185. https://doi.org/10.1002/jpln.201500472

Raison, R. J., Khanna, P. K., & Woods, P. V. (1985). Transfer of elements to the atmosphere during low-intensity prescribed fires in three Australian subalpine eucalypt forests. *Canadian Journal of Forest Research*, *15*(4), 657–664. https://doi.org/10.1139/x85-107

Reed, S. C., Townsend, A. R., Taylor, P. G., & Cleveland, C. C. (2011). Phosphorus cycling in tropical forests growing on highly weathered soils. *Phosphorus in Action: Biological Processes in Soil Phosphorus Cycling*, *26*, 339–369. https://doi.org/10.1007/978-3-642-15271-9_14

Rodrigues, J. L. M., Pellizari, V. H., Mueller, R., Baek, K., Jesus Eda, C., Paula, F. S., Mirza, B., Hamaoui, G. S., Jr., Tsai, S. M., Feigl, B., Tiedje, J. M., Bohannan, B. J., & Nüsslein, K. (2013). Conversion of the Amazon rainforest to agriculture results in biotic homogenization of soil bacterial communities. *Proceedings of the National Academy of Sciences of the United States of America*, *110*(3), 988–993. https://doi.org/10.1073/pnas.1220608110

Romanya, J., Khanna, P. K., & Raison, R. J. (1994). Effects of slash burning on soil-phosphorus fractions and sorption and desorption of phosphorus. *Forest Ecology and Management*, *65*(2–3), 89–103. https://doi.org/10.1016/0378-1127(94)90161-9

Sanchez, P. A. (1977). Properties and management of soils in the tropics. *Soil Science*, *124*(3), 187.

Silva-Olaya, A. M., Mora-Motta, D. A., Cherubin, M. R., Grados, D., Somenahally, A., & Ortiz-Morea, F. A. (2021). Soil enzyme responses to land use change in the tropical rainforest of the Colombian Amazon region. *PLoS One*, *16*(8), e0255669. https://doi.org/10.1371/journal.pone.0255669

Sinsabaugh, R. L., & Shah, J. J. F. (2010). Integrating resource utilization and temperature in metabolic scaling of riverine bacterial production. *Ecology*, *91*(5), 1455–1465. https://doi.org/10.1890/08-2192.1

Sinsabaugh, R. L., & Shah, J. J. F. (2012). Ecoenzymatic stoichiometry and ecological theory. *Annual Review of Ecology, Evolution, and Systematics*, *43*(43), 313–343. https://doi.org/10.1146/annurev-ecolsys-071112-124414

Soltangheisi, A., de Moraes, M. T., Cherubin, M. R., Alvarez, D. O., de Souza, L. F., Bieluczyk, W., Navroski, D., Teles, A. P., Pavinato, P., Martinelli, L., Tsai, S., & de Camargo, P. B. (2019). Forest conversion to pasture affects soil phosphorus dynamics and nutritional status in Brazilian Amazon. *Soil and Tillage Research*, *194*, 104330. https://doi.org/10.1016/j.still.2019.104330

Sparks, D. L., Page, A., Helmke, P., Loeppert, R., Soltanpour, P., Tabatabai, M., & Sumner, M. (1996). *Methods of soil analysis. Part 3—Chemical methods*. Soil Science Society of America Inc.

Spohn, M., & Kuzyakov, Y. (2013). Distribution of microbial- and root-derived phosphatase activities in the rhizosphere depending on P availability and C allocation—Coupling soil zymography with C-14 imaging. *Soil Biology & Biochemistry*, *67*, 106–113. https://doi.org/10.1016/j.soilbio.2013.08.015

Stone, M. M., & Plante, A. F. (2014). Changes in phosphatase kinetics with soil depth across a variable tropical landscape. *Soil Biology and Biochemistry*, *71*, 61–67. https://doi.org/10.1016/j.soilbio.2014.01.006

Tabatabai, M. A., Garcia-Manzanedo, A. M., & Acosta-Martinez, V. (2002). Substrate specificity of arylamidase in soils. *Soil Biology & Biochemistry*, *34*(1), 103–110. https://doi.org/10.1016/S0038-0717(01)00162-6

Turner, B. L., & Haygarth, P. M. (2005). Phosphatase activity in temperate pasture soils: Potential regulation of labile organic phosphorus turnover by phosphodiesterase activity. *Science of the Total Environment*, *344*(1–3), 27–36. https://doi.org/10.1016/j.scitotenv.2005.02.003

Turner, B. L., McKelvie, I. D., & Haygarth, P. M. (2002). Characterisation of water-extractable soil organic phosphorus by phosphatase hydrolysis. *Soil Biology and Biochemistry*, *34*(1), 27–35. https://doi.org/10.1016/S0038-0717(01)00144-4

Walker, T. W., & Adams, A. F. R. (1958). Studies on soil organic matter: I. Influence of phosphorus content of parent materials on accumulations of carbon, nitrogen, sulfur, and organic phosphorus in grassland soils. *Soil Science*, *85*(6), 307–318.

Wang, X., Phillips, B. L., Boily, J.-F., Hu, Y., Hu, Z., Yang, P., Feng, X., Xu, W., & Zhu, M. (2019). Phosphate sorption speciation and precipitation mechanisms on amorphous aluminum hydroxide. *Soil Systems*, *3*(1), 20.

Wang, X., Wang, Q., Prass, M., Pöhlker, C., Moran-Zuloaga, D., Artaxo, P., Gu, J., Yang, N., Yang, X., Tao, J., Hong, J., Ma, N., Cheng, Y., Su, H., & Andreae, M. O. (2023). The export of African mineral dust across the Atlantic and its impact over the Amazon Basin. *Atmospheric Chemistry and Physics*, *23*(17), 9993–10014. https://doi.org/10.5194/acp-23-9993-2023

White, T. R., Jr., & Douthit, G. E. (1985). Use of microwave oven and nitric acid-hydrogen peroxide digestion to prepare botanical materials for elemental analysis by inductively coupled argon plasma emission spectroscopy. *Journal of the Association of Official Analytical Chemists*, *68*(4), 766–769.

Williams, P. J. (1973). Validity of application of simple kinetic analysis to heterogeneous microbial populations. *Limnology and Oceanography*, *18*(1), 159–164. https://doi.org/10.4319/lo.1973.18.1.0159

Wright, S. J. (2019). Plant responses to nutrient addition experiments conducted in tropical forests. *Ecological Monographs*, *89*(4), e01382. https://doi.org/10.1002/ecm.1382

Xu, S. W., & Arai, Y. (2022a). Adsorption mechanisms of inositol hexakisphosphate in the presence of phosphate at the amorphous aluminum oxyhydroxide-water interface. *Science of the Total Environment*, *837*, 155525. https://doi.org/10.1016/j.scitotenv.2022.155525

Xu, S. W., & Arai, Y. (2022b). Competitive sorption and accumulation of organic phosphorus in phosphate-rich soils and sediments. *Advances in Agronomy*, *173*(173), 337–374. https://doi.org/10.1016/bs.agron.2022.02.006

Yao, Q., Li, Z., Song, Y., Wright, S. J., Guo, X., Tringe, S. G., Tfaily, M. M., Paša-Tolić, L., Hazen, T. C., Turner, B. L., Mayes, M. A., & Pan, C. (2018). Community proteogenomics reveals the systemic impact of phosphorus availability on microbial functions in tropical soil. *Nature Ecology & Evolution*, *2*(3), 499–509. https://doi.org/10.1038/s41559-017-0463-5

Zhao, Q., Zeng, D. H., Fan, Z. P., & Lee, D. K. (2008). Effect of land cover change on soil phosphorus fractions in Southeastern Horqin Sandy Land, Northern China. *Pedosphere*, *18*(6), 741–748. https://doi.org/10.1016/S1002-0160(08)60069-7

Zheng, T. T., Sun, Z. X., Yang, X. F., & Holmgren, A. (2012). Sorption of phosphate onto mesoporous gamma-alumina studied with in-situ ATR-FTIR spectroscopy. *Chemistry Central Journal*, *6*(1), 1–10. https://doi.org/10.1186/1752-153x-6-26

Zhu, M., Northrup, P., Shi, C., Billinge, S. J. L., Sparks, D. L., & Waychunas, G. A. (2013). Structure of sulfate adsorption complexes on ferrihydrite. *Environmental Science & Technology Letters*, *1*(1), 97–101. https://doi.org/10.1021/ez400052r

SUPPORTING INFORMATION

Additional supporting information can be found online in the Supporting Information section at the end of this article.

How to cite this article: Xu, S., Gu, C., Rodrigues, J. L. M., Li, C., Bohannan, B., Nüsslein, K., & Margenot, A. J. (2023). Soil phosphorus cycling across a 100-year deforestation chronosequence in the Amazon rainforest. *Global Change Biology*, *30*, e17077. https://doi.org/10.1111/gcb.17077